Photonic integrated devices and functions on hybrid polymer platform

Moritz Kleinert*[a], David de Felipe[a], Crispin Zawadzki[a], Walter Brinker[a], Jung Han Choi[a], Philipp Reinke[a], Magnus Happach[a], Simon Nellen[a], Martin Möhrle[a], Heinz-Gunter Bach[a], Norbert Keil[a], Martin Schell[a]
[a]Fraunhofer Heinrich Hertz Institute, Einsteinufer 37, 10587 Berlin, Germany

ABSTRACT

Photonic devices and new functions based on HHI's hybrid integration platform PolyBoard are presented providing low-loss thin-film-element-based light routing, an on-chip micro-optical bench and mechanically flexible chips comprising optical and electrical waveguides. The newly developed transfer and integration of graphene layers enables the fabrication of active optoelectronic devices in the intrinsically passive polymer waveguide networks with bandwidths in the GHz range. These novel functionalities in combination with the mature thermo-optic components of the PolyBoard platform such as tunable lasers, switches and variable attenuators pave the way towards new applications of photonic integrated circuits in communications and sensors.

Keywords: Integrated optics, polymer waveguides, tunable lasers, graphene

1. INTRODUCTION

Photonics holds great promises for a wide array of applications. This ranges from data and telecommunications, where the use of optical data transmission is already abundant, to sensor and analytic applications, where integrated optical technologies are still sparsely deployed. However, both areas face challenges due to the ever increasing data traffic in existing network infrastructure and datacenters, as well as the demand for small and accurate sensor technologies, respectively. Especially the mega-trend towards the Internet-of-Things (IoT) is a driving force behind both developments, so that these two previously disjoint areas converge at an increasing rate.

The demand for high-speed data transmission at ever more discrete sites and the real-world implementation of novel optical sensor concepts that have previously only demonstrated their potential in laboratory settings require photonic chips with various functionalities in order to adapt to the various challenges posed by the diverse applications. Such functionalities may be realized based on discrete classical optical elements, but the use of this approach is often limited by the material and assembly costs, the required size of the free-space optics, as well as its susceptibility to mechanical shock. The key to addressing these issues is the photonic integration of optical functionalities on chip level.

Examples for monolithic integration of optical and optoelectronic functionalities on a single chip are silicon-on-insulator- (SOI) and indium phosphide (InP)-based material systems [1, 2]. In contrast, hybrid photonic integration platforms usually employ a passive material system for wave-guiding purposes and rely on semiconductor components only for photon generation and detection. Prominent representatives of this approach are the silicon nitride-based TriPleX platform as well as HHI's polymer-based PolyBoard platform [3, 4]. A chip assembly is intrinsically required for active hybrid photonic integrated circuits (PICs), in contrast to the monolithic approach. However, a fiber-chip coupling and module assembly is required in any case, reducing the relative advantage of the monolithic approach. Furthermore, due to the more complex processes involved the upfront development costs of monolithic PICs tend to be significantly higher, which is often prohibitive for the use of integrated optics in novel fields. Additionally, hybrid integration offers the possibility to use the best suiting component for the desired function. In this way, it becomes feasible to use e.g. special photodetectors and light sources on one hybrid PIC, which could not be integrated monolithically due to semiconductor growth and fabrication restrictions.

*moritz.kleinert@hhi.fraunhofer.de; phone +49 30 31002-380; hhi.fraunhofer.de

The PolyBoard platform relies on the ZPU12-RI material system by ChemOptics Ltd., which consists of UV curable perfluorinated acrylates and offers refractive index contrasts Δn between waveguide core and cladding in the range of 0.005 and 0.030. The simple spin-coating processes of the liquid uncured resin and the process temperatures below 200°C allow for the flexible hetero-integration of various materials into the polymer waveguide network. HHI has expanded its hybrid polymer platform with highly efficient thermo-optic devices [5, 6], compact thin-film-element (TFE) based filtering structures [7] and U-grooves for passive fiber-chip coupling with sub-µm precision [4], enabling the fabrication of colorless transceivers for access networks [8], coherent receivers with integrated tunable local oscillators [9] and reconfigurable multi-flow transmitters for next-generation 1 Tb/s data-center communications [10].

In order to meet the needs of emerging applications for PICs that often differ from the standard requirements for data and telecommunications, novel functionalities such as TFE-based light routing, the integration of micro-optical elements, flexible PICs and the integration of two-dimensional materials have been added to the platform recently and will be presented in this paper.

2. NOVEL FUNCTIONALITIES

2.1 Thin-film-element based low-loss light routing

Using a low refractive index contrast of $\Delta n = 0.005$ is advantageous in several aspects. First of all, the mode field diameter of the ground mode matches very well to the standard single-mode fiber (SMF). This results in fiber-chip coupling losses of below 0.1 dB and an efficient passive coupling using integrated U-grooves [4]. Furthermore, the losses induced by unguided light propagation in etched slots for TFEs with widths between 10 µm and 25 µm are significantly lower than in higher refractive index contrasts. This offers great potential for the use of PICs in highly loss-sensitive applications such as in-link monitoring systems in passive optical networks. However, bending radii in this refractive index contrast cannot go below 20 mm, comparable to SMF. It is hence desirable to avoid waveguide bends altogether because these increase the chip costs via the chip size as well as the transmission losses via the greater light path length.

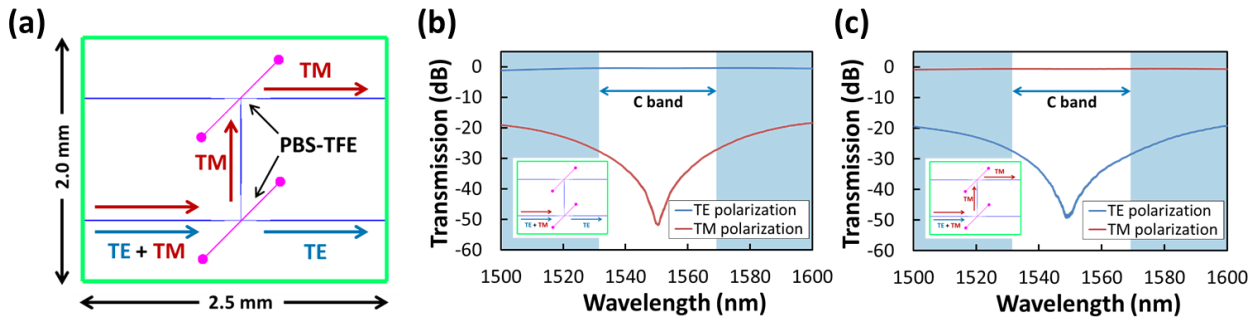

Figure 1. Sketch of the TFE-based light routing with 90° bends integrated in low refractive index contrast PolyBoard (a). (b) shows the spectrum of the non-deflected light path, while (c) shows the spectrum of the deflected light. All spectra include the total chip loss incl. fiber-chip coupling losses.

TFE-based light routing can be a way to overcome these problems while at the same time offering advanced light filter characteristics. Figure 1 (a) shows the sketch of a TFE-based light routing structure in $\Delta n = 0.005$. In the presented structure, the TFE consists of a polarizing beam splitter realized by an appropriately designed stack of dielectric layers. These PBS-TFEs were inserted perpendicular to the waveguide layer into 13 µm wide etched slots in the fabricated chip and fixed with UV-curable epoxy. Under 45° incidence angles, the TE polarized component of the light is transmitted straight through the PBS-TFE and collected in the lower output waveguide. The TM polarized light component on the other hand is reflected by the PBS-TFE and hence deflected by 90°. For measurement purposes a second PBS-TFE structure is added, deflecting the TM polarized light again by 90° into the upper output waveguide.

The spectrum in Figure 1 (b) shows the insertion loss for the non-deflected TE polarization. The losses shown here include the fiber-chip coupling losses, the propagation losses as well as the PBS-TFE losses. The maximum insertion loss across the C band is 0.7 dB, while the polarization extinction ratio (PER) is greater than 26 dB. The losses for the TM polarization in the upper output waveguide amount to maximal 0.5 dB with a PER greater 25 dB.

With TFEs, the bending radii could be reduced from 20 mm down to some tens of micrometers, while the PIC size is only limited by the TFE dimension. The corresponding bend loss can be extracted from the measured spectra due to the known coupling loss (0.1 dB per facet) and the propagation loss values (0.1 dB). One 90° bend for the TM polarization using PBS-TFE hence induces excess losses of approx. 0.1 dB. The presented structure could be used as part of a polarization diversity network in coherent receiver modules or as a simple routing structure in a transmitting PIC comprising a TM emitting laser source. By exchanging the PBS-TFE with wavelength-filtering-TFEs, the functionality can easily be adapted to the application-specific needs. A pure routing capability can also be realized with metalized TFEs acting as a conventional mirror. Hence, the low-loss TFE-based light routing opens up new flexibilities in the design of low index contrast PICs.

2.2 Integrated micro-optical bench

Although many optical functions can already be realized in integrated optics, some applications still rely on discrete optical components due to costs, performance parameters, or the sheer lack of waveguide-integrated alternatives. These include, among others, athermal etalons for wavelength stabilization of tunable lasers and magneto-optic elements for non-reciprocal functions such as optical isolators and circulators. In order to incorporate these free-space optical elements into PICs, the same integrated U-grooves structures, as used for the passive fiber-chip coupling, are employed.

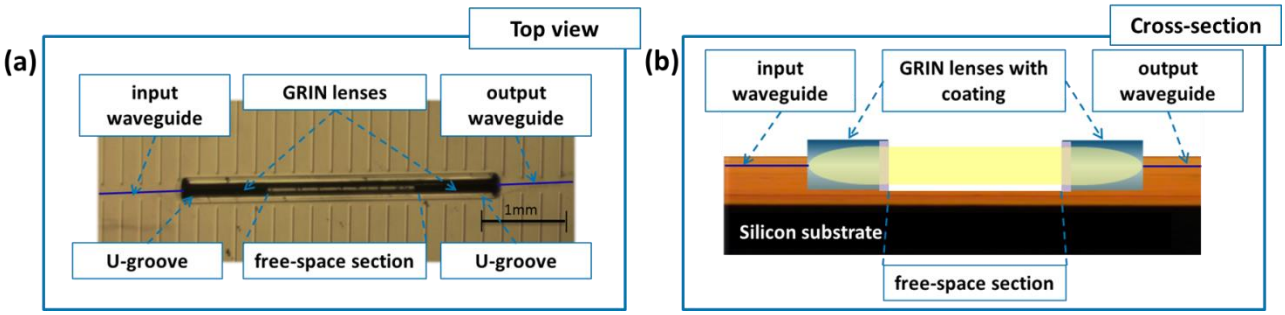

Figure 2. Micrograph (top view) of an on-chip integrated free-space section realized with GRIN lenses (a). The schematic of the cross-section (not to scale) is shown in (b). The polymer waveguide cores are accentuated in dark blue for clearer visibility.

Figure 2 (a) shows the top view and (b) the schematic cross-section of an on-chip free-space section fabricated in PolyBoard. The beam is collimated by two GRIN lenses. Both lenses are fixed with UV-curable epoxy. The 125 µm diameter of the GRIN lenses is identical to the SMF diameter. The U-grooves allow for adjustment free inserting of both GRIN lenses and SMF fibers into the PolyBoard. This is important in order to keep the later production costs as low as possible.

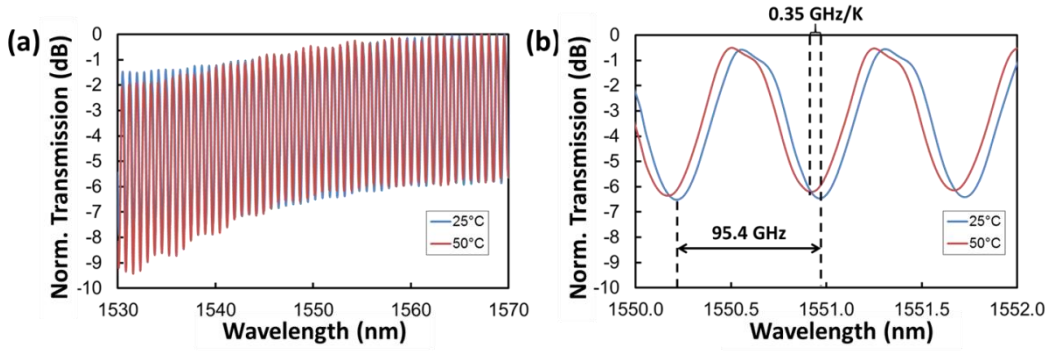

Figure 3. Transmission spectra at 25°C and 50°C through an on-chip free-space etalon with 95.4 GHz FSR across the C band (a) and between 1550 nm and 1552 nm (b).

Figure 3 shows the transmission spectrum normalized to the minimal transmission losses across the C band through an on-chip free-space section as shown in Figure 2. In order to realize a free-space etalon, the air-facing facets of the GRIN lenses were coated with dielectric layers to achieve a reflectivity of 40%. The resulting 1.57 mm long resonator features a free spectral range (FSR) of 95.4 GHz and extinction ratios of ca. 6 dB. The advantage of using air as the optical

medium in the resonator is the low temperature dependence of the resonance positions of 0.35 GHz/K. This temperature-insensitive integrated free-space etalon can be used as a stable frequency reference, e.g. in on-chip wavelength lockers for polymer-based tunable lasers [11]. By increasing the length of the free-space region slightly, a 100 GHz FSR, matching the respective ITU-T standard grid, may be realized.

Despite using etalons, micro-optical elements can be integrated, as the light beam is collimated between the GRIN lenses. Especially promising are magneto-optical crystals that allow for non-reciprocal phase shift under magnetic fields and therefore are key features of optical isolators and circulators. By offering an integrated micro-optical bench, PolyBoard enables the development of future PICs with on-chip isolator and circulator functionalities that pave the way for novel applications, e.g. in interrogators for Fiber-Bragg-Grating networks for structural health monitoring and wearable devices.

2.3 RF and optical flexlines

Flexible electronics is an active research topic especially in the area of consumer electronics. But also for data and telecommunications as well as sensor applications, flexible radio frequency (RF) electrical transmission lines and optical waveguides can be advantageous. Wearable optoelectronic sensors with integrated waveguide networks for data acquisition and flexible RF antennas might only be one example out of the emerging realm of the IoT. In contrast to brittle inorganics-based photonic integration platforms, polymers are usually more flexible making them an ideal candidate for these applications.

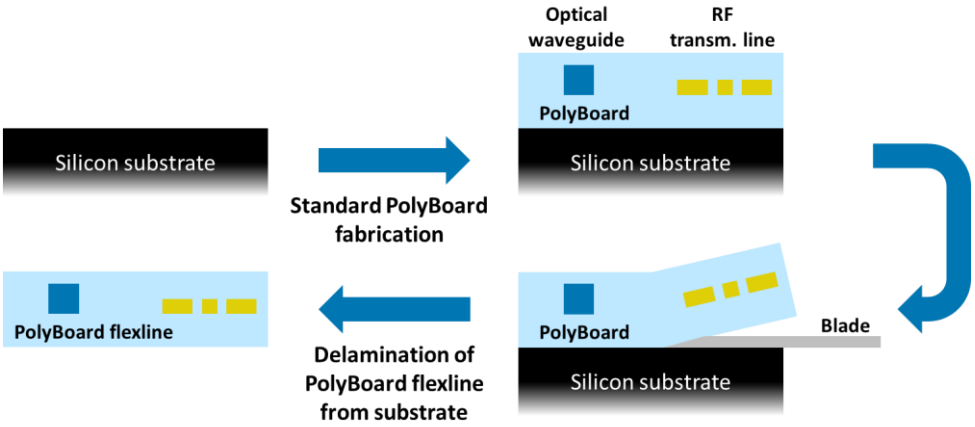

Figure 4. Fabrication process of RF and optical flexlines in PolyBoard platform by delamination from substrate.

Figure 4 shows a schematic of the work flow involved in the processing of RF and optical flexlines. The fabrication starts with a silicon wafer acting as a mechanical substrate for the subsequent polymer and metal layers. As the only differences between a standard PolyBoard process and the flexline process is the pretreatment of the substrate surface and the omission of adhesion promoters, all structures that are part of the PolyBoard platform can directly be incorporated into flexlines. After the wafer-scale fabrication, the structures are separated into single chips by dicing or dry etching and delaminated from the substrate by means of a blade. The resulting flexlines are some tens of micrometers thick, and their surface area is only limited by the wafer size of the silicon substrate.

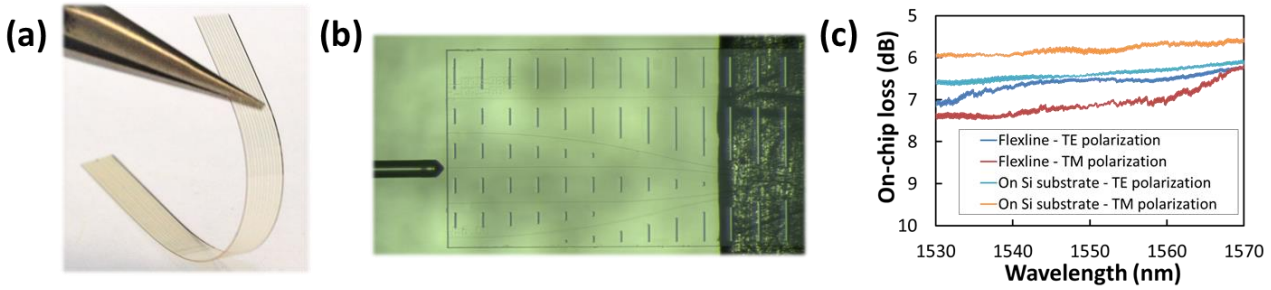

Figure 5. Photograph of an optical flexline with straight waveguides (a) and micrograph of the fiber-to-chip coupling into a 4x4 MMI flexline chip (b). (c) shows the on-chip losses for the TE and TM polarization before and after delamination for the transmission from the lowest input waveguide to the lowest output waveguide.

The losses induced by bending of the flexline as shown in Figure 5 (a) should be comparable to bend losses in the waveguide plane. Hence, for a refractive index contrast of Δn = 0.030 bend radii of 1.5 mm could be possible and are hence likely only limited by the point of mechanical failure of the chip. Figure 5 (b) shows the fiber-chip coupling into an optical flexline chip consisting of an 4x4 multimode interference (MMI) coupler realized in Δn = 0.011. The transparency of the polymer material in the visible wavelength range is easily recognizable. The measured on-chip losses [Figure 5 (c)] of this structure show different behaviors of TE and TM polarization before and after delamination. The losses of max. 6.6 dB across the C band on Si substrate for the TE polarization correspond to excess losses of max. 0.6 dB, taking the intrinsic 6 dB splitting loss of the 4x4 MMI into account. After delamination, the excess losses increase by 0.4 dB to 1.0 dB in the worst case. For the TM polarization on the other hand the losses increase by 1.4 dB. This polarization-dependence can be attributed to the phase-sensitivity of MMIs. The relaxation and slight bending of the flexline after delamination induce a birefringent behavior as the effective refractive index of the TM polarization is changed while the TE polarized light remains largely unaffected. Therefore, the use of phase sensitive components on optical flexline PICs should be restricted to the TE polarization. Non-phase-sensitive functions, such as TFEs and thermo-optic devices can be integrated without further prerequisites.

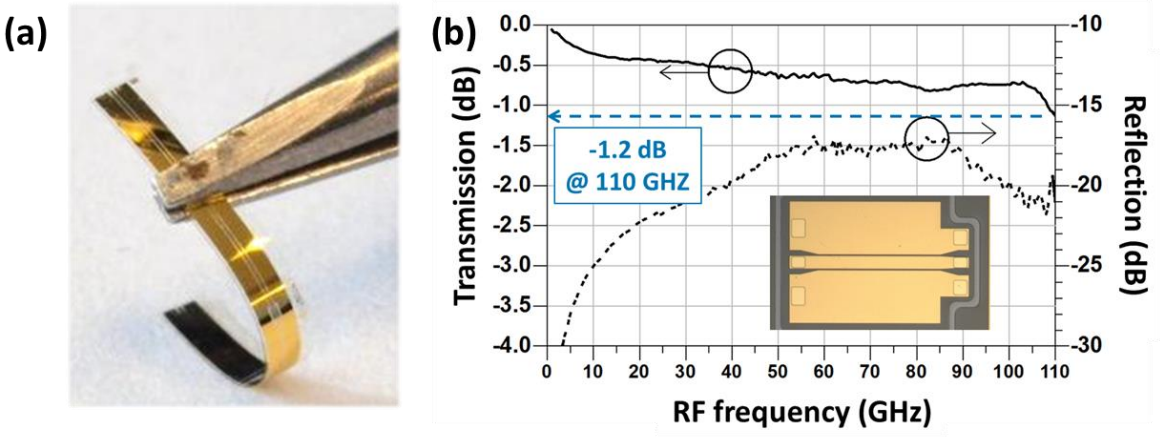

Figure 6. Photograph of a bent RF flexline (a) and measured transmission and reflection up to 110 GHz for a 1 mm long CPW RF flexline (b). The inset shows the top view of a fabricated CPW structure.

Similar to optical flexlines, mechanically flexible RF transmission lines can be realized in PolyBoard as demonstrated in Figure 6 (a). Figure 6 (b) shows the frequency-dependence of the transmission and reflection through a 1 mm long coplanar waveguide (CPW). Up to 110 GHz, the attenuation increases to max. 1.2 dB, indicating a 3-dB bandwidth well above 110 GHz. The reflection of the electrical signal stays below -16 dB across the entire frequency range.

As the fabrication processes of the optical and RF flexlines shown here are compatible, both functionalities can be co-integrated on the same chip offering novel flexibilities in the design and packaging of optoelectronic integrated circuits.

2.4 Graphene-based electro-optic functionalities

The amorphous nature of the materials used for passive wave-guiding in hybrid photonic integration platforms has the advantage of cost-effective processes and high flexibility in the design of the layer stacks. However, these are optically passive and the light manipulation is usually limited to relatively slow effects such as thermo-optical and stress-optical modulation [12, 13]. This impairment can be overcome by the integration of novel two-dimensional material systems that have received a lot of research attention in recent years. The most prominent representative of this material class is graphene, a monoatomic layer of carbon atoms in a hexagonal lattice. While due to its thickness of just 0.35 nm a seamless integration into existing platforms is possible, graphene offers unique electro-optical properties that can be exploited within intrinsically passive waveguide networks. In the last two years, a graphene transfer and structuring process has been incorporated into PolyBoard that allows for the fabrication of optoelectronic devices without the need for separate semiconductor components.

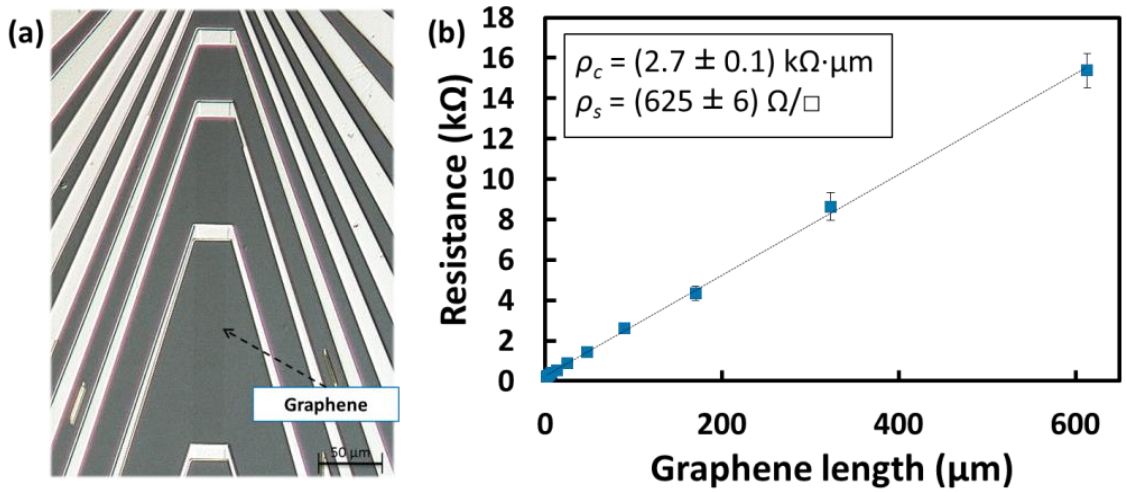

Figure 7. Micrograph (a) of a TLM structure for the deduction of contact and sheet resistance of graphene and length-dependent resistance measurements (b).

This process allows for the graphene integration on 4” wafer scale using commercially available graphene layers grown on copper foil by chemical vapor deposition and is scalable to larger wafer diameters. Figure 7 (a) shows a transmission length method (TLM) structure designed to determine the specific contact and sheet resistances ρ_c and ρ_s. The metal electrodes consist of 30 nm titanium and 120 nm gold. It should be noted that the 25 µm wide graphene stripe, structured by oxygen plasma etching, is visible in the micrograph although it is only one monolayer thin. This is due to graphene’s high optical absorption of 2.3% that is almost constant for wavelengths from the visible to the near infrared [14]. By plotting the measured resistances over the length of the respective graphene stripe as shown in Figure 7 (b), ρ_s can be calculated from the slope, while ρ_c is determined by the intercept with the ordinate axis. The contact resistance equals to (2.7 ± 0.1) kΩ·µm and the area-specific sheet resistance (625 ± 6) Ω/□. It can be seen that the slope is linear for graphene lengths up to 600 µm. From this fact as well as the value of ρ_s, we can infer that the quality of the transferred graphene on a micrometer scale is high and that the developed transfer process to the PolyBoard wafer does not induce significant defects on a millimeter scale either.

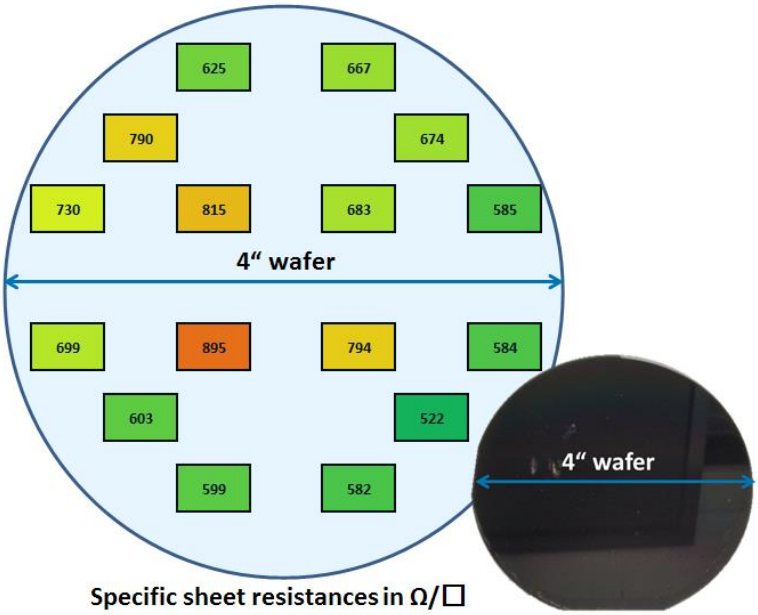

Figure 8. Specific sheet resistances of graphene transferred to a 4” PolyBoard wafer determined with TLM structures. All values are given in Ω/□. The inset shows a PolyBoard wafer after transfer of a 4” graphene sheet resulting in a coverage of >95%.

TLM structures as shown in Figure 7 are fabricated across the 4” wafer in order to assess the on-wafer reproducibility of the transfer process. Results for a representative wafer are shown in Figure 8. The specific sheet resistances range from 582 Ω/□ to 895 Ω/□ with a mean value of 678 Ω/□ and a standard deviation of 100 Ω/□. While these values already enable electro-optic devices with bandwidths in the GHz range [15, 16], great emphasis is put on the further reduction of the resistances by optimizing the transfer process and the metal-graphene ohmic contact, as the bandwidth of graphene-based devices are usually limited by their RC constant.

The integration of graphene already offers the possibility of fabricating electro-absorption modulators [17] and potentially enables the co-integration of Mach-Zehnder modulators and photodetectors with some tens of GHz bandwidth on a passive PolyBoard chip as well.

3. POLYBOARD-ENABLED DEVICES

3.1 Dual tunable laser for THz generation

The PolyBoard technology allows for the integration of hybrid dual wavelength tunable sources which can be used for the photonic generation of mm-wave and THz signals, with applications in fields such as continuous-wave THz spectroscopy systems and next-generation wireless communication networks. In Figure 9, a picture of the dual wavelength device is shown, comprising a dual InP gain element operating as a gain medium and two polymer Bragg gratings which serve as tunable wavelength-selective mirrors to form two DBR cavities. The wavelengths of the Bragg gratings are designed to be 1550 nm (DBR 1) and 1568 nm (DBR 2) at room temperature. Both lasers are combined on-chip by means of a polymer waveguide Y-branch. The wavelength tuning of the device is based on the thermo-optical (TO) effect, which is achieved by micro-heater electrodes placed nearby the polymer Bragg reflectors. By increasing the current applied on the heater electrodes, and hence increasing the temperature, tuning of the Bragg wavelength to shorter wavelengths occurs due to the negative TO coefficient (TOC) of the polymer material (-10^{-4}/K). An additional thermo-optical phase shifter on the polymer chip allows for fine adjustment of wavelength and side-mode suppression ratio (SMSR). The fairly high TO coefficient (TOC) of the polymer material, in combination with its low thermal conductivity, provide an efficient wavelength tuning mechanism.

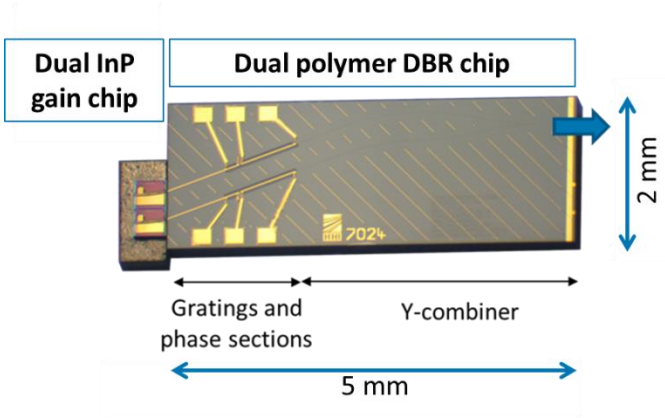

Figure 9. Photograph of the hybrid integrated polymer/InP dual DBR device, comprising a dual InP gain element and a polymer chip with thermo-optically tunable phase shifters and Bragg gratings (DBRs).

For the application of tunable wavelength sources in continuous-wave (CW) THz spectroscopy systems, the mode-hop-free tunability is a crucial feature in order to perform scans over broad frequency ranges for the detection of absorption lines of different gases. Figure 10 (a) shows the THz scan that has been performed by means of mode-hop-free tuning of each one of the DBR lasers in counter wavelength directions over a range of more than 4.5 nm for each laser [18]. This provides a complete scan of more than 1.2 THz, enabling the detection of different H_2O absorption resonances due to the air humidity. However, by means of optimizing the laser cavity, mode-hop-free tuning ranges as wide as 9 nm have been demonstrated [18], showing the potential for achieving scans of more than 2 THz in CW spectroscopy systems.

In order to evaluate the performance of the proposed source for highly-resolved THz spectroscopy, the dual tunable laser source was continuously tuned with very high resolution to perform THz sweeps in the range between 1.090 THz and 1.223 THz. In Figure 10 (b), the comparison of the measured THz signal using the polymer-based dual tunable laser and commercially available external cavity laser diodes (ECDLs) is presented. The vertical dashed lines indicate different H_2O absorption lines. As it can be observed, the measured amplitude using the dual polymer/InP device overlaps well with the measurement results obtained with a commercially available ECDL and several H_2O absorption lines can be well resolved. The obtained results, together with the potential of achieving scans of more than 2 THz, demonstrate the potential of the proposed PolyBoard-based structure for its use in CW THz spectroscopy systems.

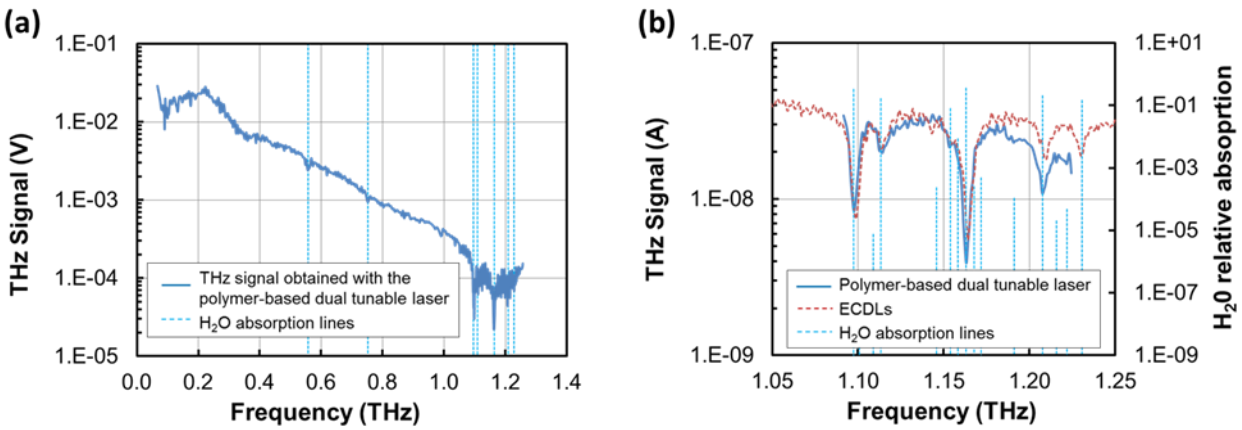

Figure 10. (a) Broadband CW THz scan achieved by means of photomixing using the dual tunable laser as mode-hop-free optical source and comparison between the polymer-based dual tunable laser and commercially available ECDLs in a highly resolved THz scan for detecting water in air (b).

Regarding the field of THz wireless communications, the polymer-based dual tunable laser has demonstrated to be an inexpensive optical source for the flexible photonic generation of the THz carriers [19]. Free running beat-notes with a linewidth of a few MHz have been obtained without any stabilization scheme or phase locking, being comparable to the best case for monolithically integrated dual DFB lasers [19]. This work can potentially pave the way towards hybrid

microwave photonic transmitters comprising mode-locked lasers for phase locking of the polymer-based dual wavelength source, graphene-based modulators for the generation of the data stream, photodetector arrays for photomixing of the optical signals, and high frequency antennas using polymer as a substrate, similar to the RF flexlines, to radiate the THz waves.

3.2 Graphene-based electro-absorption modulators

The transfer and structuring process of high-quality graphene layers on 4"-wafer scale as outlined in section 2.4 enables the fabrication of active optoelectronic components within the passive waveguide material system of the PolyBoard platform. As the optical absorption within a graphene layer is tunable with an external voltage, electro-absorption modulators (EAMs) are promising examples of graphene-based optoelectronic functionalities and have been realized in silicon-on-insulator as well as polymer waveguide platforms [15–17].

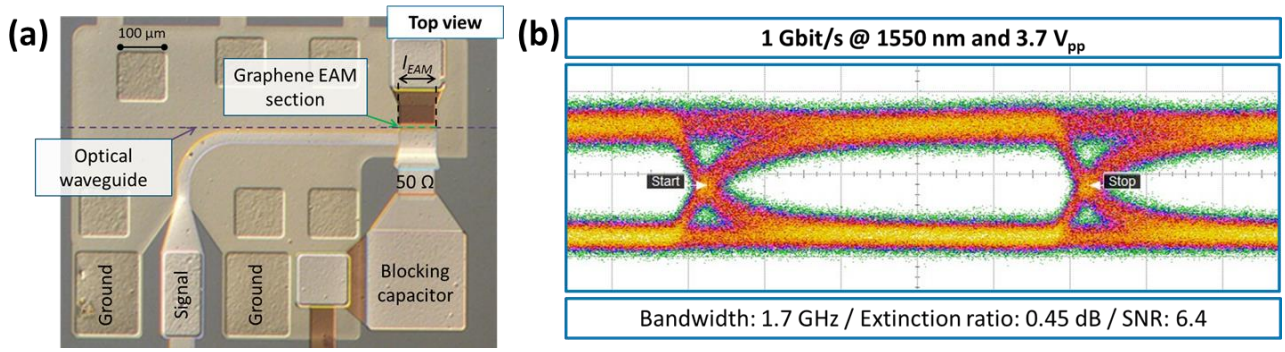

Figure 11. (a) shows a micrograph of a GP-EAM before deposition of the top electrical ground plane. The position of the polymer optical waveguide and the active EAM section are highlighted with dashed purple and green lines, respectively. An eye diagram of a 100 µm long GP-EAM device at 1 Gbit/s is shown in (b).

The spin-coating processes involved in the PolyBoard fabrication and the low dielectric constant of 2.7 of the polymer material allow for the co-integration of complex electrical networks with the graphene-polymer EAMs (GP-EAMs) as shown in Figure 11 (a). The ground-signal-ground configuration enables the transmission of electrical signals in the GHz range from the RF input pads to the active EAM section. The electrical transmission line is terminated with a 50 Ω resistor for impedance matching as well as a DC blocking capacitor in order to be able to apply a DC bias offset to the graphene layers.

Figure 11 (b) shows an eye diagram measurement on a fabricated 100 µm long GP-EAM at a data rate of 1 Gbit/s. At a modulation voltage of 3.9 V_{pp} an extinction ratio of 0.45 dB and a signal-to-noise ratio (SNR) of 6.4 were achieved. While the current GP-EAM optimization work focusses on the increase of the 3dB-modulation bandwidth to more than 25 GHz and the extinction ratio to about 10 dB, the presented device's bandwidth of 1.7 GHz demonstrates the speed potential of the GP-EAMs that can be integrated with all other functionalities of the PolyBoard toolbox. Especially the low wavelength dependence of the electro-optic properties of the graphene layers for wavelengths between 400 nm and 2000 nm in combination with the low refractive index contrast of the polymer waveguide offers new opportunities in sensing and analytic applications.

4. CONCLUSION AND OUTLOOK

The implementation of novel functionalities, such as low-loss TFE-based light routing, integrated micro-optical benches and graphene-based optoelectronics into the PolyBoard platform in combination with its well-established precise U-grooves for passive fiber-chip coupling, TFE-based filters and efficient TO devices offers great potential for future cost-effective and highly integrated PICs for communications and sensor applications. Especially the possibility to realize flexible optical components on the basis of the mature on-chip functionalities without the need for a profound re-design can proof ground-breaking. It enables the fabrication of wearable devices and the application of photonics for novel sensor concepts that rely on the interaction of the optical chip with the environment paving the way towards an ever more connected world driven by the Internet-of-Things.

ACKNOWLEDGEMENTS

This work was partly conducted in the framework of the PolyPhotonics Berlin and Phonograph projects, both sponsored by the German Federal Ministry of Education and Research (BMBF) and co-financed by the European Commission under the projects EU FP-7 PANTHER and EU H2020 HAMLET.

REFERENCES

[1] Lim, A. E.-J., Song, J., Fang, Q., Li, C., Tu, X., Duan, N., Chen, K. K., Tern, R. P.-C. and Liow, T.-Y., "Review of Silicon Photonics Foundry Efforts," IEEE J. Select. Topics Quantum Electron. 20(4), 405–416 (2014).

[2] Smit, M., Leijtens, X., Ambrosius, H., Bente, E., van der Tol, J., Smalbrugge, B., Vries, T. de, Geluk, E.-J., Bolk, J., van Veldhoven, R., Augustin, L., Thijs, P., D'Agostino, D., Rabbani, H., Lawniczuk, K., Stopinski, S., Tahvili, S., Corradi, A., Kleijn, E., Dzibrou, D., Felicetti, M., Bitincka, E., Moskalenko, V., Zhao, J., Santos, R., Gilardi, G., Yao, W., Williams, K., Stabile, P., Kuindersma, P., Pello, J., Bhat, S., Jiao, Y., Heiss, D., Roelkens, G., Wale, M., Firth, P., Soares, F., Grote, N., Schell, M., Debregeas, H., Achouche, M., Gentner, J.-L., Bakker, A., Korthorst, T., Gallagher, D., Dabbs, A., Melloni, A., Morichetti, F., Melati, D., Wonfor, A., Penty, R., Broeke, R., Musk, B. and Robbins, D., "An introduction to InP-based generic integration technology," Semicond. Sci. Technol. 29(8), 83001 (2014).

[3] Wörhoff, K., Heideman, R. G., Leinse, A. and Hoekman, M., "TriPleX: A versatile dielectric photonic platform," Advanced Optical Technologies 4(2), 189–207 (2015).

[4] Kleinert, M., Zhang, Z., Felipe, D. d., Zawadzki, C., Maese Novo, A., Brinker, W., Möhrle, M. and Keil, N., "Recent progress in InP/polymer-based devices for telecom and data center applications," Proc. SPIE 93650, 93650R (2015).

[5] Felipe, D. d., Zhang, Z., Brinker, W., Kleinert, M., Novo, A. M., Zawadzki, C., Möhrle, M. and Keil, N., "Polymer-Based External Cavity Lasers. Tuning Efficiency, Reliability, and Polarization Diversity," IEEE Photon. Technol. Lett. 26(14), 1391–1394 (2014).

[6] Maese-Novo, A., Zhang, Z., Irmscher, G., Polatynski, A., Mueller, T., Felipe, D. d., Kleinert, M., Brinker, W., Zawadzki, C. and Keil, N., "Thermally optimized variable optical attenuators on a polymer platform," Appl. Opt. 54(3), 569–575 (2015).

[7] Felipe, D. d., Kleinert, M., Zawadzki, C., Brinker, W., Goebel, T., Möhrle, M. and Keil, N., "Recent Developments in the Polymer Photonic Integration Technology," Advanced Photonics 2016 (IPR, NOMA, Sensors, Networks, SPPCom, SOF), ITu3A.1 (2016).

[8] Zhang, Z., Felipe, D. d., Brinker, W., Kleinert, M., Novo, A. M., Zawadzki, C., Möhrle, M. and Keil, N., "Bi-directional, crosstalk-suppressed, 40-nm wavelength tuneable colourless ONU on polymer platform," ECOC, 1–3, (2014).

[9] Zhang, Z., Novo, A. M., Polatynski, A., Mueller, T., Irmscher, G., Felipe, D., Kleinert, M., Brinker, W., Zawadzki, C. and Keil, N., "Colorless, Dual-Polarization 90° Hybrid with Integrated VOAs and Local Oscillator on Polymer Platform," Optical Fiber Communication Conference, Th1F.3 (2015).

[10] Keil, N., Felipe, D., Zhang, Z., Kleinert, M., Zawadzki, C., Brinker, W., Polatynski, A., Irmscher, G., Möhrle, M., Bach, H.-G. and Schell, M., "Novel Integration Technologies for Disruptive Capacity Upgrade in Data Centre Systems," Optical Fiber Communication Conference, Th3F.3 (2016).

[11] Felipe, D. d., Happach, M., Kleinert, M., Zawadzki, C., Brinker, W., Rehbein, W., Möhrle, M., Keil, N., Hofmann, W. and Schell, M., "Polymer-based Integrated Tuneable Laser with On-Chip Wavelength Locker," ECOC, 1-3 (2016).

[12] Hosseini, N., Dekker, R., Hoekman, M., Dekkers, M., Bos, J., Leinse, A. and Heideman, R., "Stress-optic modulator in TriPleX platform using a piezoelectric lead zirconate titanate (PZT) thin film," Opt. Express 23(11), 14018–14026 (2015).

[13] Zhang, Z. and Keil, N., "Thermo-optic devices on polymer platform," Optics Communications 362, 101–114 (2016).

[14] Mak, K. F., Ju, L., Wang, F. and Heinz, T. F., "Optical spectroscopy of graphene. From the far infrared to the ultraviolet," Solid State Communications 152(15), 1341–1349 (2012).

[15] Hu, Y., Pantouvaki, M., van Campenhout, J., Brems, S., Asselberghs, I., Huyghebaert, C., Absil, P. and Van Thourhout, D., "Broadband 10 Gb/s operation of graphene electro-absorption modulator on silicon," Laser & Photonics Reviews 10(2), 307–316 (2016).
[16] Liu, M., Yin, X. and Zhang, X., "Double-layer graphene optical modulator," Nano letters 12(3), 1482–1485 (2012).
[17] Kleinert, M., Herziger, F., Reinke, P., Zawadzki, C., Felipe, D. d., Brinker, W., Bach, H.-G., Keil, N., Maultzsch, J. and Schell, M., "Graphene-based electro-absorption modulator integrated in a passive polymer waveguide platform," Opt. Mater. Express 6(6), 1800 (2016).
[18] Felipe, D. de, Happach, M., Nellen, S., Brinker, W., Kleinert, M., Zawadzki, C., Möhrle, M., Keil, N., Göbel, T., Petermann, K. and Schell, M., "Hybrid polymer/InP dual DBR laser for 1.5 μm continuous-wave terahertz systems," Proc. SPIE 9747, 974719 (2016).
[19] Carpintero, G., Hisatake, S., Felipe, D. d., Guzman, R., Nagatsuma, T., Keil, N. and Gobel, T., "Photonics-based millimeter and terahertz wave generation using a hybrid integrated dual DBR polymer laser," IEEE MTT-S International Microwave Symposium (IMS), 1–3 (2016).